

Phase Synchronization for the Recognition of Mental Tasks in a Brain–Computer Interface

Elly Gysels and Patrick Celka

Abstract—Brain–computer interfaces (BCIs) may be a future communication channel for motor-disabled people. In surface electroencephalogram (EEG)-based BCIs, the extracted features are often derived from spectral estimates and autoregressive models. We examined the usefulness of synchronization between EEG signals for classifying mental tasks. To this end, we investigated the performance of features derived from the phase locking value (PLV) and from the spectral coherence and compared them to the classification rates resulting from the power densities in α , β_1 , β_2 , and 8–30-Hz frequency bands.

Five recordings of 60 min, acquired from three subjects while performing three different mental tasks, were analyzed offline. No artifacts were removed or rejected. We noticed significant differences between PLV and mean spectral coherence. For sole use of synchronization measures, classification accuracies up to 62% were achieved. In general, the best result was obtained combining phase synchronization measures with α power spectral density estimates. The results demonstrate that phase synchronization provides relevant information for the classification of spontaneous EEG during mental tasks.

Index Terms—Brain–computer interface (BCI), phase synchronization, surface electroencephalogram (EEG).

I. INTRODUCTION

BRAIN–COMPUTER interfaces (BCIs) allow for communication and control that does not depend on the brain's normal output channels of peripheral nerves and muscles [1]. Their users can actually control cursor movement, direct a wheelchair, select letters or icons on a computer screen, or operate a neuroprosthesis [2]. The main interest of this research is to develop a communication channel for persons with severe motor disabilities [3].

In surface electroencephalogram (EEG)-based interfaces, very often spectral estimates [4], [5] and autoregressive (AR) coefficients [6], [7] and measures derived from them [8] are used to characterize the EEG. Some authors exploit spatial information by considering multivariate autoregressive models (MVARs) [6], temporal and spatial complexity measures [9], common spatial patterns (CSPs) [10], or joint time–frequency–space correlation (TFSC) [11]. In this paper, we examine yet another measure that quantifies interaction between EEG signals and has a more direct neurophysiological

interpretation: the phase locking value (PLV). We compare it to spectral coherence, another widely-used measure of synchronization.

Different regions widely distributed over the brain must communicate to provide the basis for integration of sensory information and for many functions that are critical for learning, memory, information processing, perception, and behavior of organisms. Transient periods of synchronization of oscillating neuronal discharges have been proposed to act as an integrative mechanism that may bring a widely distributed set of neurons together into a coherent ensemble that underlies a cognitive act. Rodriguez *et al.* [12] demonstrated a direct participation of synchrony in a cognitive task.

Many studies employ spectral coherence to quantify synchronization processes in the brain, e.g., [13]–[16]. Recently, Delorme and Makeig [17] studied power and coherence changes in EEG data recorded from a highly trained subject during sessions in which he attempted to regulate power at 12 Hz over his left- and right-central scalp. They observed changes in partial phase coherence between maximally independent components.

The PLV is a time-domain synchronization measure frequently applied in recent EEG analysis. It was first described by Hoke *et al.* [18] for magnetoencephalography as Phase Coherence (R). In 1999, it was introduced in electroencephalography by Lachaux *et al.* [19] as PLV and, in 2000, by Mormann *et al.* [20] as R in the fields of cognitive neuroscience and epilepsy research, respectively. Since then, this measure has been used in a variety of studies, e.g., [21]–[29].

Quiroga *et al.* [30] applied several linear and nonlinear measures of synchronization to three typical EEG signals. Mutual information was not robust due to the low number of data points. The other measures, namely, nonlinear interdependences, phase synchronizations, cross correlation, and the coherence function, all resulted in a useful quantification of synchronization. Separation between synchronization levels was more pronounced with nonlinear measures, but qualitative results were the same. It was concluded that these measures are valuable for the study of synchronization in real data.

To our knowledge, the PLV and spectral coherence have not yet been applied to classify EEG in the framework of BCIs. In this study, both spectral coherence and PLV will be used to distinguish EEG recorded during three mental tasks.

The following are the purposes of this paper:

- 1) investigate whether synchronization measures are suitable for classifying mental tasks in a BCI;
- 2) make a first comparison of the performances of PLV and mean spectral coherence;

Manuscript received September 23, 2003; revised September 27, 2004. This work was supported by the Swiss National Science Foundation through the National Centre of Competence in Research on Interactive Multimodal Information Management (IM2).

E. Gysels is with the Swiss Center for Electronics and Microtechnology, Neuchâtel, CH-2007 Switzerland (e-mail: elly.gysels@csem.ch).

P. Celka is with the Gold Coast Campus, School of Engineering, Griffith University, Brisbane, Qld. 9726, Australia.

Digital Object Identifier 10.1109/TNSRE.2004.838443

- 3) make a first comparison of the performances of synchronization measures and power spectral density estimates.

The paper is constructed as follows. In Sections II and III, the experimental setup and the data preprocessing are described. Subsequently, in Section IV, we introduce PLV and spectral coherence. Section V explains the features and feature subsets that have been considered for this study. Section VI is about the employed classifier. Finally, the results are reported in Section VII and discussed in Section VIII.

II. EEG RECORDING AND EXPERIMENTAL PARADIGM

Five healthy right-handed volunteers (two women and three men), aged between 22 and 33, took part in the experiments. No selection criteria were used. None of the subjects had participated in BCI experiments before. For each subject, a total of 60 min of EEG was recorded in five sessions of 4 min/day, on three consecutive days. The sessions were separated by breaks of 5–10 min. Subjects were seated comfortably in front of a computer. They were asked not to move during the sessions and look at the computer screen.

About every 20 s, the operator informed the subject which new task they have to perform. The mental tasks to be done, with opened eyes, were imagination of repetitive self-paced left hand movement (“left”) and imagination of repetitive self-paced right-hand movement (“right”). The imagined hand movement was a flexion at the wrist causing the hand moving up and down. The third task, also done with eyes opened, “word,” consisted of generating words that begin with the same letter, freely chosen by the subject. The words were not spoken. The three tasks were alternated randomly and such that the incidence of the three tasks was equal.

Most BCIs follow a synchronous protocol [4], [5], [31], which generates predetermined control periods during which the user can respond. A stimulus sequence usually comprises of a warning message, followed a few seconds later by a stimulus. Subjects are required to do the mental task only after hearing and/or seeing the stimulus.

In our protocol, no cue was used. Subjects switched about every 20 s randomly between the three mental tasks. In such a protocol, not only must it be determined which mental task is being performed, but also when it is being performed. The communication, however, is more “natural” as the users can spontaneously switch between tasks. The advantage is not to be dependent on external triggers and to have, thus, a potentially faster system. In this paper, we deal with resolving the mental task corresponding to an EEG window.

EEG signals are recorded with the 32-channel Biosemi ActiveTwo system (<http://www.biosemi.com>). Electrodes were placed on the scalp according to the 10–20 international electrode placement system. The ground electrode is replaced by two separate electrodes. They form a feedback loop, decreasing the effective impedance with a factor of 100 at 50 Hz. The 32 electrodes are shown in Fig. 3, as well as the two electrodes replacing the reference electrode. EEG signals were digitized at a sampling rate $f_s = 2048$ Hz, subsampled to $f_s = 512$ Hz and stored for offline analysis. No filtering was performed prior to digitizing. Together with the EEG signals, we recorded the

“task signal,” indicating which task the subject is doing at every moment.

For the purpose of introducing and studying new features, we performed an offline study of data recorded without feedback. In this condition, the subjects cannot adapt to any features or classification algorithms used to provide the feedback.

III. DATA PREPROCESSING

If the mental task changed, the corresponding 1-s window and its subsequent window were removed from the recorded EEG data. For each day of recording, about 1050 windows remained available for classification.

A. Artifacts

To study how many artifacts occurred and to which extent they were still present in the frequency band used in this study, the raw and 8–30-Hz filtered EEG were visually inspected for artifacts.

Ocular artifacts occurred in signals recorded from Fp1, Fp2, AF3, and AF4 in 15.55%, 11.80%, and 10.34% of the windows for day one, two, and three, of recording from subject 1. More artifacts occurred during the task “word.” Subject 2 presented artifacts in 4.99%, 13.52%, and 2.37% of the windows. For subject 3, artifacts occurred in 4.56%, 3.18%, and 2.22% of the windows on day one, two, and three, respectively. The raw EEG of subjects 4 and 5 presented ocular artifacts in 9.95%, 4.22%, and 3.88% and in 4.39%, 2.04%, and 11.90% of the windows on days one, two, and three, respectively. The percentage of windows containing artifacts did not differ more than 2.5% for the three different tasks, except for subject 3, day two, and subject 5, day three, where more artifacts occurred during the task “left” and “word,” respectively.

Inspection of the EEG bandpass filtered in 8–30 Hz, the frequency band considered in this study, showed that these artifacts were mostly filtered out. Indeed, ocular artifacts generally appear under 4 Hz [32].

Muscle artifacts were present in the EEG of subject 3 for four sessions of day one and three sessions of day two. They appear on channels F7, T7, F8, and T8 during long periods, covering the three different tasks. For one session of day three of recording from subject 5, three consecutive windows out of 69 windows coinciding with the task “word” contained muscle artifact.

The muscle artifacts occurred during the three tasks. In addition, most of their energy is not contained in the 8–30 Hz frequency band considered here [32].

Automatic EEG artifact detection and rejection/removal techniques (see [32]–[34] and references therein) have been developed to process long-term EEG recordings, to improve evoked potential studies where the corruption of a few seconds of EEG turns out to be critical, or for systems where automated EEG preprocessing is necessary.

Considering spontaneous EEG signals, three situations can occur. First, if the artifact occurrence rate (AOR) is low, and artifacts thus have no or few impact on the analysis, it is not worth the effort to detect and reject or remove them. Second, if the AOR is high, artifact rejection/removal would remove most of the EEG information content. Third, if the AOR is in

between the two previous situations, artifact rejection/removal could be of interest. Still, removing artifacts is a very delicate task because the information content of the spontaneous EEG is widely spread in the space and frequency domain. Hence, removal would certainly distort or destroy the brain activity present in the EEG. The best solution is, thus, a simple rejection of the artefact.

In most sessions considered in our study, the AOR was quite low (few percents). For seven sessions of subject 3, the muscle AOR was quite high. As it was not necessary to exclude artifacts to be sure of classifying brain activity, and because AOR in different sessions was either very low or very high, we decided not to treat them any further.

B. Preprocessing Synchronization Features

A linear phase FIR 8–30-Hz bandpass filter was applied to the EEG before computing the synchronization measures (PLV and mean spectral coherence). This was done because, for comparison, we wanted to derive PLV and coherence based features from the same signals and with the same prior knowledge.

Simulations on sinusoidal signals with noise showed that computing PLV from an unfiltered, noisy signal still distinguished periods of different coupling. The coherence, averaged over the whole spectrum, however, did not. Filtering or taking the average over a limited frequency band was necessary to distinguish periods of common activity from others. We refer to Section IV-C.

The 8–30-Hz frequency band was chosen because it contains the μ and β rhythms, which have been proved to be involved in motor-tasks [4].

C. Preprocessing Power Features

Before calculating power features, a Laplacian filter was applied, followed by the same bandpass filter as applied to the computation of the synchronization features. The surface Laplacian was computed from a spherical spline interpolation scheme [35], [36]. Its application to the scalp surface potential was motivated by the fact that it has been shown to be an estimate of the cortical surface potential, which is a more accurate estimation of the cortical activity than the surface EEG.

IV. PHASE LOCKING VALUE AND SPECTRAL COHERENCE

The EEG signals are analyzed using a sliding window $w(N)$ of N samples. Each EEG signal is divided into M windows, experimentally determined from the length of the signal.

A. Phase Locking Value

The PLV characterizes the stability of the phase differences between the phases $\varphi_x(t)$ and $\varphi_y(t)$ of two signals $s_x(t)$ and $s_y(t)$ across subsequent time samples of one window as follows:

$$\text{PLV} = \left| \left\langle e^{j\Delta\varphi(t)} \right\rangle \right| \quad (1)$$

where $\Delta\varphi(t) = \varphi_y(t) - \varphi_x(t)$ and $\langle \cdot \rangle$ is the averaging operator. For the discrete case, it suffices to replace t by k/f_s , $k = 1, \dots, N$. PLV equals the length of the sum vector of all unit vectors $e^{j\Delta\varphi(t)}$ in one window, divided by the number

of samples in that window. When the phase difference is constant (phase synchronization), all phase difference vectors will be aligned, resulting in a PLV equal to 1. If the phase differences are randomly distributed over $[0, 2\pi]$, the vector sum, and thus the PLV, will be 0.

To compute the PLV, we first need to know the instantaneous phase $\varphi(t)$. To this end, we employ the Hilbert transform.

The Hilbert transform finds its origin in the fact that, for causal signals, a relation between the real and imaginary parts of the Fourier transform of the signal exists. In the ideal case the Hilbert transform is a $\pi/2$ -degree phase shifter. Thus, e.g.,

$$s_e(t) = \cos(2\pi ft + \phi)$$

transforms into

$$\tilde{s}_e(t) = \sin(2\pi ft + \phi).$$

The Hilbert transform of $s(t)$ is given by

$$\tilde{s}(t) = \frac{1}{\pi} p.v. \int_{-\infty}^{+\infty} \frac{s(\tau)}{t - \tau} d\tau \quad (2)$$

p.v. denoting the Cauchy principal value, and allows us to determine the instantaneous phase φ_s as follows:

$$\varphi_s(t) = \arctan \left(\frac{\tilde{s}(t)}{s(t)} \right). \quad (3)$$

The application of the Hilbert transform to nonstationary signals and its interpretation are discussed in [37].

A significant improvement in computation time was achieved with the following algorithm.

- Compute the Hilbert transform of the signals $s_x(t)$ and $s_y(t)$ and construct the analytical signals

$$\begin{aligned} S_x(t) &= s_x(t) + j\tilde{s}_x(t) \\ S_y(t) &= s_y(t) + j\tilde{s}_y(t). \end{aligned}$$

- Instead of explicitly computing the phase of both signals as in (3), we normalize the analytical signals

$$\begin{aligned} S_{xn}(t) &= \frac{s_x(t) + j\tilde{s}_x(t)}{s_x^2 + \tilde{s}_x^2(t)} \\ S_{yn}(t) &= \frac{s_y(t) + j\tilde{s}_y(t)}{s_y^2 + \tilde{s}_y^2(t)}. \end{aligned}$$

From this, we can directly derive $e^{j\Delta\varphi(t)}$

$$\begin{aligned} e^{j\Delta\varphi(t)} &= \cos(\varphi_y(t) - \varphi_x(t)) + j \sin(\varphi_y(t) - \varphi_x(t)) \\ &= \text{Re}(S_{yn}(t)) \text{Re}(S_{xn}(t)) + \text{Im}(S_{yn}(t)) \text{Im}(S_{xn}(t)) \\ &\quad + j (\text{Im}(S_{yn}(t)) \text{Re}(S_{xn}(t)) \\ &\quad - \text{Re}(S_{yn}(t)) \text{Im}(S_{xn}(t))). \end{aligned}$$

In the discrete case, the Hilbert transform [38] is computed by the so-called discrete-time analytic signal. Integrals are replaced by sums.

B. Spectral Coherence

The spectral coherence of two signals $s_x(t)$ and $s_y(t)$ is the squared normalized cross-power spectrum

$$K_{XY}^2(f) = \frac{|\langle C_{XY}(f) \rangle|^2}{\langle C_{XX}(f) \rangle \langle C_{YY}(f) \rangle} \quad (4)$$

where $C_{XY}(f) = X(f)Y^*(f)$, $C_{XX}(f) = X(f)X^*(f)$, $C_{YY}(f) = Y(f)Y^*(f)$, $X(f)$, and $Y(f)$ are the Fourier transforms of $s_x(t)$ and $s_y(t)$. The spectral coherence, like the PLV, has a value between 0 and 1. A coherence value of 1 means that the corresponding frequency components of the signals $s_x(t)$ and $s_y(t)$ are identical, except for a multiplicative amplitude difference and a constant time relation (phase delay). Practically, for finite length, signals it means that both signals are related by a linear transform. A 0 coherence indicates that the corresponding frequency components of both signals are not correlated.

To obtain a scalar value from $K_{XY}^2(f)$, the average coherence in some frequency band ΔB , i.e., $\langle K_{XY}^2(f) \rangle_{\Delta B}$, as well as the maximum or minimum coherence values, can be considered.

For the EEG studies described in this paper, we used the average coherence with $\Delta B = 8\text{--}30$ Hz, after filtering the signal in the frequency band 8–30 Hz. Using the maximum of the coherence spectrum did not yield good results, probably due to the fact that there is always some common activity present in the EEG signals.

C. Properties of PLV and Spectral Coherence

Simulations on sinusoidal signals suggest that the time resolution of PLV is better than that of coherence. We considered two sinusoidal signals that had a frequency component in common in one interval

$$s_x(t) = \cos(2\pi 13t) + \cos(2\pi 22t) + \sigma\zeta(t) \quad \forall t$$

$$s_y(t) = \begin{cases} \cos(2\pi 6t) + \sigma\zeta(t) & \forall t = \frac{1}{f_s} \dots \frac{t_{\text{tot}}}{3} \\ \cos(2\pi 13t) + \sigma\zeta(t) & \forall t = \frac{t_{\text{tot}}}{3} + \frac{1}{f_s} \dots \frac{2t_{\text{tot}}}{3} \\ \cos(2\pi 17t) + \sigma\zeta(t) & \forall t = \frac{2t_{\text{tot}}}{3} + \frac{1}{f_s} \dots t_{\text{tot}} \end{cases}$$

where $\sigma\zeta(t)$ is a Gaussian white noise with variance σ^2 and t_{tot} is the total time (30 s). $f_s = 512$ Hz in these simulations.

When decreasing the window length, the interval of common activity is distinguished less clearly, see Fig. 1. The PLV and the averaged coherence (Coh) are shown, respectively. The plots show synchronization values, derived from windows of 128, 256, and 512 samples, respectively, as a function of time. For very short time windows, Coh does not distinguish different intervals of common activity. PLV does, although with great variability. Increasing the window length decreases the variance and increases the difference in synchronization values for the different regimes.

The variability originates from the fact that Fourier transforms are performed on fractional periods of the signals, which creates phase jumps. Adding noise smooths this effect.

Fig. 2 shows PLV and Coh after adding gaussian white noise to the signals in 50 Monte Carlo runs. It can be seen that Coh averaged over the whole spectrum should not be used without filtering.

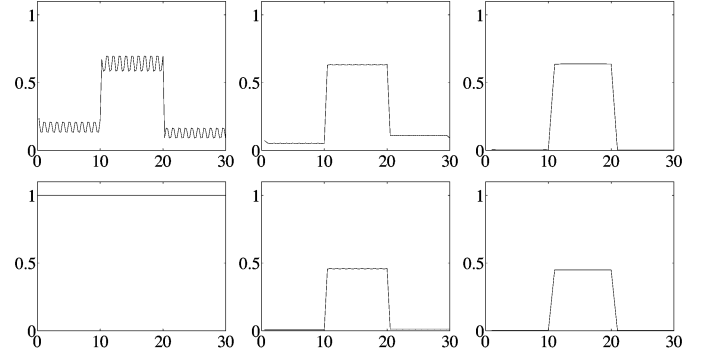


Fig. 1. Influence of window length on (top) PLV and (bottom) Coh, $\sigma = 0$. From left to right, window length equals 128, 256, 512, samples, respectively.

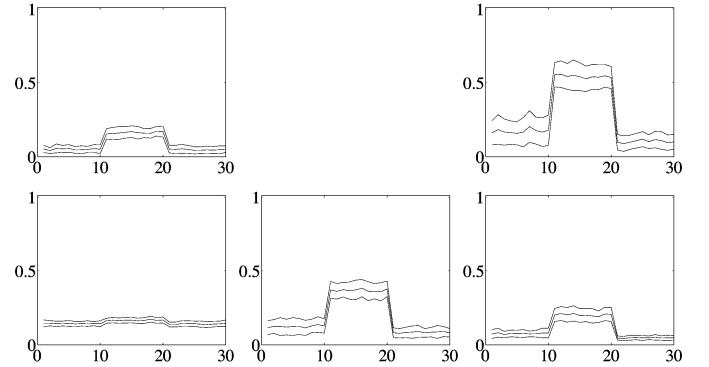


Fig. 2. (Top) Mean(PLV), \pm standard deviation, after adding noise to the signals. (Bottom) Mean(Coh), \pm standard deviation, after adding noise to the signals. From left to right: $\sigma = 1$, no filtering, Coh with $\Delta B = 0\text{--}256$ Hz; $\sigma = 1$, no filtering, Coh with $\Delta B = 8\text{--}30$ Hz; $\sigma = 1$, filtering between 8–30 Hz, Coh with $\Delta B = 0\text{--}256$ Hz.

The computation time is considerably smaller for PLV than for coherence, if calculation of PLV is implemented as in Section IV-A.

V. FEATURES

This paper is aimed at directly evaluating the classification performance of different (groups of) features, in order to compare PLV with mean spectral coherence and synchronization with power features.

Considering twice 496 electrode pairs together with power features in a few frequency bands would result in a huge amount of features, making a comparison of these features very difficult. Therefore, we define different features from the pair-wise synchronization measures in Section V-A. Additional features are defined from power spectral density estimates in Section V-B. Finally, for the actual comparison of the different types of features, 53 different subsets of the set of features at disposition were considered (Section V-C).

A. Synchronization Based Features

We propose different PLV and Coh based features, that assess the interaction between EEG brain activity recorded at neighboring electrodes. We studied general levels of synchronization in different regions (Section V-A1), the coupling between signals recorded from an electrode and its neighbors

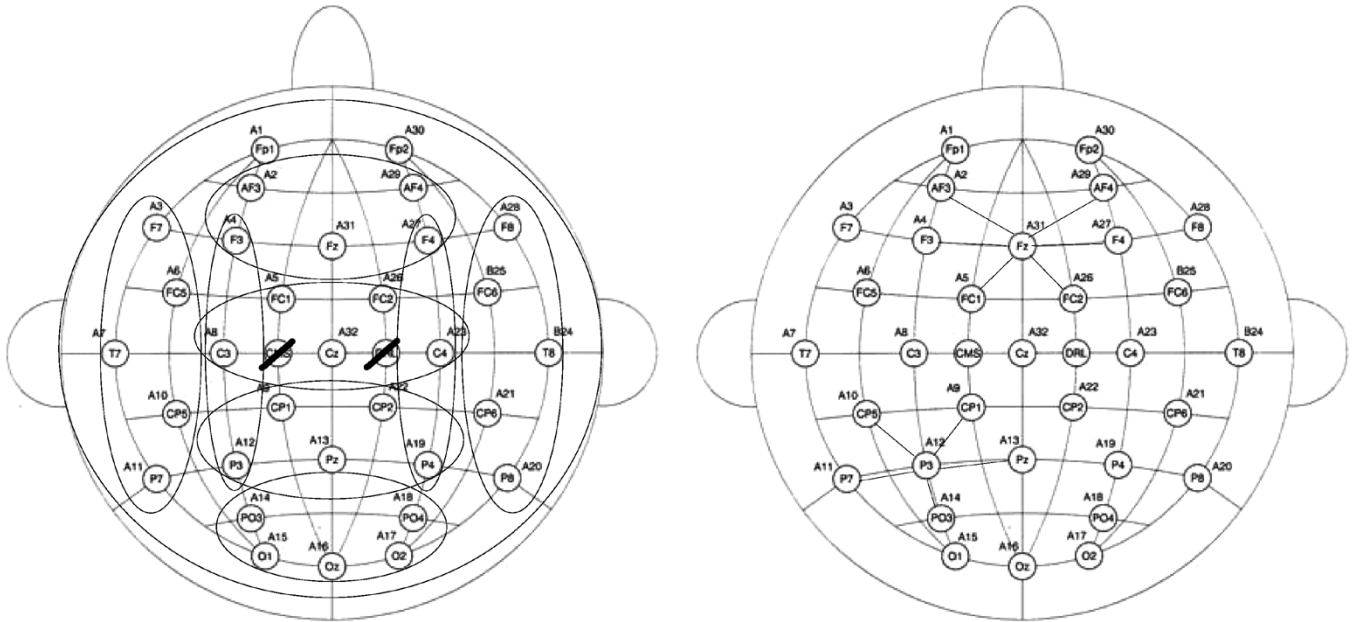


Fig. 3. Illustration to the synchronization features computed from the EEG signals. See text for details.

(Section V-A2), and a few of the individual electrode pairs (Section V-A3).

PLV and Coh were computed from sliding 1-s windows, eight times per second, in the frequency band 8–30 Hz. The length of 1s was chosen arbitrarily. The shorter the windows, the less accurate the estimation of the features, while longer windows make the system react slower.

To compute the discrete Hilbert transform, the number of samples for fast Fourier transform, N_{fft} , was set to $f_s * 1s$. For computing the coherence, parameters were set as follows: N_{fft} was $2 * f_s * 1s$; a Hanning window of length $N_{\text{fft}}/8$ was used; the overlap was $(N_{\text{fft}}/16) - 1$.

We computed PLV and Coh for all 496 electrode pairs and then derived the following features.

1) *Group Averages*: Nine averages over, respectively, the PLV and Coh values of all possible electrode pairs within a group of electrodes were considered. These nine group averages are illustrated in the left panel of Fig. 3. One value represented the average over all possible electrode pairs, indicating a general level of synchronization. Furthermore, six averages for a “frontal” (AF3, AF4, F3, Fz, F4), “central” (FC1, FC2, C3, Cz, C4), “parietal” (CP1, CP2, P3, Pz, P4), “occipital” (PO3, PO4, O1, Oz, O2), “left” (F7, T7, P7, FC5, CP5), and “right” (F8, T8, P8, FC6, CP6) group were obtained. Two more values resulted from averaging over the pairs F3-C3, F3-P3, and C3-P3 on the one hand and F4-C4, F4-P4, and C4-P4 on the other hand.

2) *Interaction With Neighbors*: Furthermore, each electrode was attributed two values corresponding to the averaged PLV and Coh values of the electrode pairs formed by this electrode and its neighbors. The right panel of Fig. 3 shows an example for two electrodes.

3) *Details in the Fronto-Centro-Parietal and Temporal Region*: At last, 40 synchronization values between individual electrode pairs in the fronto-centro-parietal region (formed with electrodes F3, C3, P3, Fz, Cz, Pz, F4, C4, P4) were considered, for both PLV and Coh, because of the involvement of this part

of the cortex in the motor tasks. Unfortunately, this electrode placement has only one electrode in the temporal region, which is involved in language tasks. Therefore, we included the synchronization values between the signals recorded at electrodes T7-FC5, T7-CP5, T8-FC6, and T8-CP6.

This specific choice of averages and individual electrode pairs was arbitrary, but symmetrical. It relied on the one hand on physiological information regarding motor and language tasks, on the other hand we wanted to reduce the number of features that would result from considering all possible electrode pairs and enhance their relevance by combining certain of them. In fact, in cognitive neuroscience there are often just one or a few electrode pairs considered, or all pairs are summed.

B. Band Power Estimates

The power spectral densities (PSDs) in the α (8–12 Hz), β_1 (13–18 Hz), and β_2 (19–30 Hz) frequency bands, as well as the PSD in the larger band 8–30 Hz, which we will denote with λ , were computed for the 32 EEG signals by means of the Welch’s averaged PSD estimate from 1-s sliding windows, eight times per second. N_{fft} was set to $f_s * 1s/2$, the overlap to $N_{\text{fft}}/2$. A Hanning window of length N_{fft} was used.

As the classifier needs numbers of the same order of magnitude at its input, every power feature was rescaled by dividing it by the average over all power features of the same type at the same time instance. The same procedure was applied to the PLV and Coh features.

C. Subsets of Features

With the total of 162 synchronization features (81 PLV and 81 Coh) and 128 power features, 53 different groups of features, called subsets, were constructed and tested on the available data. Some subsets consisted of one type of feature only (PLV, Coh, α , β_1 , β_2 , and λ PSD features), other subsets combined PSDs with synchronization based features. The PSD features or the

TABLE I
RESULTS FOR AND TYPES OF FEATURES CONTAINED IN BEST FEATURE SUBSETS FOR THE RESPECTIVE SUBJECTS AND DAYS OF RECORDING

Subject Day	Subject 1			Subject 3			Subject 5		
	1	2	3	1	2	3	1	2	3
CR (%)	57.55	63.15	67.81	64.49	63.33	62.58	55.14	46.38	52.77
UR (%)	5.89	7.25	6.77	7.51	6.88	8.32	6.44	8.73	7.63
Type	PLV	α	$PLV + \alpha$	$Coh + \alpha$	$Coh + \lambda$	$Coh + \alpha$	PLV	PLV	$PLV + \beta_1$

TABLE II
CLASSIFICATION ACCURACIES (%) FOR SOLE USE OF SYNCHRONIZATION AND POWER SPECTRAL DENSITY FEATURES

Subject Day	Subject 1			Subject 3			Subject 5		
	1 (CR/UR)	2 (CR/UR)	3 (CR/UR)	1 (CR/UR)	2 (CR/UR)	3 (CR/UR)	1 (CR/UR)	2 (CR/UR)	3 (CR/UR)
Only PLV	57.55/5.40	62.35/5.49	60.95/4.58	57.31/6.70	60.81/5.02	56.94/4.81	55.14/6.45	46.38/8.09	50.91/6.41
Only Coh	48.23/11.17	54.79/9.69	52.10/10.54	57.87/8.92	58.86/8.48	52.13/9.89	40.28/9.07	34.11/10.41	39.40/11.60
Only α	49.33/10.99	63.15/7.24	65.05/7.24	62.64/8.54	58.03/7.36	60.54/8.97	48.97/8.69	38.76/10.50	44.22/9.95
Only β_1	42.09/10.51	53.58/8.15	56.66/8.06	43.89/10.53	47.15/10.51	48.99/9.24	48.41/8.70	40.24/6.69	45.84/8.00
Only λ	45.71/11.07	61.53/6.88	63.32/7.96	52.34/9.03	59.70/8.19	59.80/7.58	48.12/8.04	42.65/8.64	47.66/8.47

synchronization measures at single electrodes, as defined in Section V-A2, were considered at all electrodes or only at C and P electrodes (C3, Cz, C4, P3, Pz, P4). In addition, a combination of synchronization values for individual electrode pairs in the fronto-centro-parietal region was considered, as well as their combination with α power features at the C and P electrodes.

A detailed description of all of the 53 subsets would lead us too far, but, as an example, the best performing subsets will be described in detail in Section VII-B.

VI. CLASSIFICATION

The classifier consisted of a combination of three support vector machines (SVMs) with a linear kernel. Each individual SVM was trained with data from two tasks only: “left” and “right,” “left” and “word,” and “right” and “word.” For distinguishing the three mental tasks of the test set, the classification results of the three trained SVMs were combined to obtain the final class (“left,” “right,” or “word”) or a label “unknown.”

Features were computed from 1-s sliding windows with (7/8)(s) overlap and classified. Every second, strict majority voting was applied to the eight classification results to determine the class. If no strict majority was attained, the window was categorized as ‘unknown’.

The data were studied per day and per subject by means of five-fold cross-validation, using four sessions for training and the fifth one for testing. Each of the five sessions was test set once.

VII. RESULTS

In this section, we present the results from our experiments. We will first discuss some general observations for the five subjects in Section VII-A. In Section VII-B, we show the classification accuracies for the best subsets and describe these subsets in more detail. Section VII-C illustrates the sole use of synchronization and power features, respectively. Finally, in Section VII-D, the different types of features are compared by means of significance tests.

The tables present, for each day and each subject, results from five-fold cross-validation. “CR” refers to the average percentage

of correctly classified windows. “UR” is the percentage of windows for which the system responds “unknown” (neither correct classification, nor mistake). The remaining percentage is the error rate.

A. Observations on the Different Subjects

From a global inspection of the performances of the five subjects, it appeared that subjects 2 and 4 did not achieve good classification results. For many subsets, classification accuracies were hardly better than random (33%). Therefore, we decided to exclude both subjects for the study and comparison of the different feature subsets.

The results for the other three subjects are presented in Tables I and II. The performance of subject 1 increases over the three days. This subject reported difficulties with imagining the hand movements the first day and felt comfortable with the task only the third day. Subject 3 performs slightly less on days two and three than on day one. We learned afterwards that this subject had a minor car accident between day one and two. Furthermore, he reported he got used to the procedure. The results achieved in case of subject 5 were better for the first day and the last one. The subject reported that he felt more attentive day one and part of day three.

B. Best Feature Subsets

Table I shows the classification results obtained for the best feature subsets for the three days of recording for each subject. In all but one case, synchronization-based measures are contained in the best performing feature subset. Four out of nine subsets contain synchronization values between individual electrode pairs. In addition, α power features, at all electrodes or just at the C and P electrodes, appear often in these subsets.

For distinguishing the three classes, the best classification accuracies achieved for the respective subjects are 67.81%, 64.49%, and 55.14%. Artifacts had no significant influence on these results. Manually rejecting artifacts resulted in CRs of 66.69%, 66.82%, and 54.39% and URs of 7.88%, 8.06%, and 6.35%, respectively.

If one had to give feedback to the subject, offline evaluation of the performance of different feature subsets on the first day of recording will be a good indicator. In our experiments, the

feature subset with the best three-day average performance was also the best feature subset on day one for two subjects. Also, the combination of synchronization with PSD features is generally one of the best feature subsets, evaluated over the different days.

Each window contains $32 * 512 = 1664$ samples, and is then characterized by a few tens of feature values. Here, follow, e.g., the details of the best features subsets, for the different subjects and the different days of recording.

- 1) Subject 1, day one and subject 5, day one: PLV values for the electrode pairs described in Section V-A3 (40 features).
- 2) Subject 1, day two: PSD in the α band, all electrodes (32 features)
- 3) Subject 1, day three: PLV, group values, and values at C and P electrodes; and PSD in the α band, all electrodes (47 features).
- 4) Subject 3, day one: Coh, group values and values at C and P electrodes; and PSD in the α band, all electrodes (47 features).
- 5) Subject 3, day two: Coh, group values and values at C and P electrodes; and PSD in the λ band, all electrodes (47 features)
- 6) Subject 3, day three: Coh values for the pairs F3-C3, F3-P3, C3-P3, Fz-Cz, Fz-Pz, Cz-Pz, F4-C4, F4-P4, and C4-P4; and PSD in the α band, at C and P electrodes (15 features).
- 7) Subject 5, day two: PLV for the electrode pairs C3-F3, C3-Cz, C3-P3, C4-F4, C4-Cz, C4-P4, P3-Pz, P4-Pz, T7-CP5, and T8-CP6 (ten features)
- 8) Subject 5, day three: PLV, group values and values at C and P electrodes; and PSD in the β_1 band, at C and P electrodes (21 features).

The PLV and Coh group values and values at individual electrodes are as defined in Sections V-A1 and V-A2, respectively.

C. Sole Use of Synchronization and Power Features

The best classification rate when using a subset of only PLV, Coh, α , β_1 , or λ features, respectively, is indicated in Table II. When using only synchronization measures, three-class distinction with accuracies up to 62.35%, 60.81%, and 55.14% was achieved for subjects 1, 3, and 5, respectively. The achievement of significant classification accuracies using only synchronization features demonstrates their usefulness.

When using only α -power estimates, the maximum accuracies were 65.05%, 62.68%, and 48.97%. Sole use of λ -power estimates resulted in maximum classification rates of 63.32%, 59.80%, and 48.12% for the three respective subjects.

When using synchronization and power features separately for classifying the three mental tasks, PLV outperforms the power-subsets on the three days for subject 5 and on one day for subjects 1 and 3. The other two days for subjects 1 and 3, α -power features perform better.

D. Significance Tests

A total of 23 pairs of feature subsets were compared with one another to test for significant differences between PLV and Coh, between the different power features, between power features

TABLE III
DIFFERENCES BETWEEN SYNCHRONIZATION AND POWER DENSITY FEATURES FOR DIFFERENT SUBJECTS AND DIFFERENT DAYS. (S)B (S)W: FIRST TYPE OF FEATURE IS (SIGNIFICANTLY) BETTER (WORSE) THAN THE ONE BEHIND SLASH. LEVEL OF SIGNIFICANCE: 0.05

Types tested	Subject 1			Subject 3			Subject 5		
	1	2	3	1	2	3	1	2	3
PLV / Coh	SB	-	SB	SB	SW	-	SB	SB	SB
λ / α	W	-	-	SW	-	-	-	-	SB
λ / β_1	B	SB	SB	SB	SB	SB	-	-	-
λ / β_2	SB	SB	SB	SB	SB	SB	SB	SB	SB
α / β_1	SB	SB	SB	SB	SB	SB	-	-	-
α / β_2	SB	SB	SB	SB	SB	SB	SB	SB	SB
β_1 / β_2	B	SB	SB	SB	SB	SB	SB	SB	SB
PLV / λ	B	SW	-	-	SW	SW	-	-	-
PLV / α	-	SW	-	SW	SW	SW	-	B	SB
PLV / β_1	SB	W	-	SB	-	-	-	-	-
PLV / β_2	SB	B	SB	SB	SB	SB	SB	SB	SB
Coh / λ	SW	SW	SW	SW	-	SW	SW	SW	SW
Coh / α	SW	SW	SW	SW	SW	SW	SW	SW	SW
Coh / β_1	-	SW	SW	SB	SB	-	SW	SW	SW
Coh / β_2	-	B	-	SB	SB	SB	SB	-	-
$PLV + \alpha / PLV$	B	SB	SB	SB	SB	SB	SB	SB	-
$PLV + \alpha / \alpha$	SB	-	B	-	B	-	-	SB	SB
$PLV + \lambda / PLV$	-	SB	SB	-	SB	SB	SB	-	SB
$PLV + \lambda / \lambda$	SB	-	SB	SB	SB	-	-	SB	SB
$Coh + \alpha / Coh$	SB	SB	SB	SB	SB	SB	SB	SB	SB
$Coh + \alpha / \alpha$	SB	SB	B	-	SB	-	-	-	-
$Coh + \lambda / Coh$	SB	SB	SB	SB	SB	SB	SB	SB	SB
$Coh + \lambda / \lambda$	SB	SB	-	SB	SB	-	-	B	-
$PLV + \alpha / Coh + \alpha$	B	-	-	-	-	-	-	SB	SB
$PLV + \lambda / Coh + \lambda$	-	-	SB	-	-	-	-	SB	SB

and synchronization measures, and between the combination of synchronization measures and power features and the individual subsets.

To this end, we considered the following 20 subsets. Ten subsets consisted of the PLV, Coh, α , β_1 , β_2 , λ , PLV and α , PLV and λ , Coh and α , and Coh and λ features at the 32 electrodes. Another ten subsets were constructed with these features at the C and P electrodes only. As explained in Section V-A2, the PLV or Coh value for a single electrode is the mean of the PLV or Coh values of the electrode pairs formed by this electrode and its neighbors.

The data from the different days of recording for different subjects were analyzed separately. After computation of the CRs for the five sessions, by means of five-fold cross validation, the results for the corresponding subsets with features at all electrodes and features at the six C and P electrodes only were concatenated. A pairwise student's t-test was then applied to these ten results for the two respective types of subsets that we wanted to compare.

Table III gives an overview of the results. "SB" means that the first mentioned type of feature is performing significantly better than the second one, with a level of significance ≤ 0.05 . "B" means that the first type is better than the second one, but not significantly ($0.05 < p < 0.1$). "SW" and "W" mean that the second type is the better one, and "-" means that the performance of the different types of features is not significantly different.

1) *PLV versus Coh*: For subjects 1 and 5, PLV was significantly better than Coh, for two of the three and all three days, respectively. For subject 3, PLV was significantly better on the first day, Coh was significantly better on the second day, and there was no significant difference on the third day. This shows that both measures extract different information from the signals.

2) *Power Estimates*: Other power spectral density estimates achieve significantly better classification accuracies than the

power spectral density in the β_2 band. α and λ power measures do not show a clear distinction regarding performance. For subjects 1 and 3, they are significantly better than β_1 power spectral density estimates. It is actually surprising that the α and λ power density estimates did not result in a larger difference in classification rates. The 8–30-Hz band contains apart from the relevant α band also the seemingly less relevant or even irrelevant β_2 band, which is three times larger than the α band. Only twice a significant difference between the performance of α and λ power spectral densities has been noticed.

3) *Synchronization versus Power Estimates*: The λ and α power spectral densities perform significantly better than PLV for subject 3 and significantly better than Coh for all three subjects. There was no clear difference between the performance of PLV and β_1 power spectral density estimates. The β_1 power spectral density performed significantly better than Coh for subjects 1 and 5. Coh performed significantly better than β_1 and β_2 for subject 3. PLV performed significantly better than β_2 power spectral density for the three subjects.

4) *Combination of Synchronization and Power Features*: The lower part of Table III shows that combining synchronization measures with power spectral density estimates can lead to improved results compared to classifications using the individual subsets separately.

However, conclusions about reciprocal additional information should be drawn carefully. For subject 5, day three, e.g., the fact that the subset $PLV + \alpha$ performs significantly better than α is probably due to the good performance of PLV features only. From the same table, we can see that PLV performs significantly better than α PSDs for that subject on that day.

Of interest are the cases where there is no significant difference in performance between a synchronization measure and α or λ PSD while their combination leads to significantly improved results. For example, we see that there is no significant difference in performance of PLV and λ features for subject 1 and 5 on day three, while the subset combining these features performs significantly better.

Table III also shows that for subject 3, day two, α power spectral density features achieve significantly better results than Coh features. The combination of both types of features not only performs significantly better than Coh features, but also significantly better than the α features.

We would like to emphasize that for these significance tests only the features at individual electrodes have been considered. The performance improvement yielded by the synchronization values between individual electrode pairs reported in Section V-A3 could not be considered here, as they do not have a PSD equivalent. We remark that four of the nine best subsets described in Section VII-B were subsets containing synchronization values between individual electrode pairs. To better assess the whole set of 290 features, in a future study, feature selection algorithms will be used to find the better features.

VIII. DISCUSSION

This paper presents a study on the use of synchronization measures in the framework of BCIs. The performance of the

PLV and the mean spectral coherence Coh for classifying mental tasks is evaluated. There are significant differences between these measures. In general, PLV yielded better results than Coh (see Table III). This may be because synchronization is more restrictive than coherence. The signals of two synchronized systems are correlated, but increased coherence does not necessarily imply synchronization [39].

We demonstrated that from PLV and Coh, computed from broadband signals, interesting features can be derived, containing relevant information for classification of spontaneous EEG during mental tasks. For sole use of features derived from synchronization between EEG signals, for three different subjects, classification rates of 62.35%, 60.81%, and 55.14% were obtained for distinction of the three mental tasks “left,” “right,” and “word.”

While synchronization measures computed from narrow band signals have a clearer physical interpretation, synchronization between broadband signals may be more difficult to achieve and may, therefore, be more distinctive. This issue will be investigated in future studies.

From Table III, it can be seen that α and λ features outperform β_1 features in case of subject 1 and 3 and β_2 features for all three subjects. High-frequency features are systematically worse than lower frequency or broad band features.

A comparison of synchronization and PSD features is difficult, because they are intrinsically different. While power features are computed from single EEG signals, synchronization features characterize the interaction between two EEG signals. We compared the performance of power measures with the one of synchronization features at individual electrodes, characterizing the interaction with neighbors, in a paired student’s t-test. We found that the α and λ features are significantly better than Coh for the three subjects and significantly better than PLV for subject 3. Considering their combination, however, we see that synchronization measures and power spectral density add information to each other. No combination of features is worse than the separate ones.

Since coupling features are broadband, the superior performance of subsets containing as well synchronization features as PSD features may be due to the availability of more information for the classifier. However, subsets containing as well the broadband synchronization features as broadband PSD features (λ) perform better than the separate ones. This suggests that the superior performance of sets containing features of both types is not due to the availability of more information for the classifier, but rather to the presence of coupling features.

In this comparison, group averages and individual electrode pairs are not considered. Therefore, the different types of features will be compared by means of feature selection algorithms in a future study. While only six out of the nine best subsets contained power features, eight of these subsets contained synchronization features. Four of them included group averages and four synchronization values between individual electrode pairs. Hence, we believe that the study of synchronization measures could improve current BCI systems. Further studies, employing, e.g., feature selection, are needed to confirm this. Combining synchronization and power features, for the three respective subjects, three-class classification accuracies of up

to 67.81%, 64.49%, and 55.14% were obtained. Error rates were 25.42%, 29.1%, and 39.6%. We compare our results to other results on three-class differentiation reported in literature.

Anderson [40] investigates the three mental tasks “baseline,” “letter,” and “math” for one subject and reports 85% classification accuracy when averaging over 4 0.5-s windows, overlapping with 0.25 s. Millán *et al.* [41] distinguish between the mental tasks “relax,” “left,” and “right” (no feedback). While left and right motor imagery was performed with eyes opened, “relax” was done with closed eyes. This results in a much higher recognition rate of the task “relax” (100% and 92%, respectively) than for the tasks “left” (42% and 51%) and “right” (36% and 56%). The average true positive rates reported were 52% and 63%. The merit of this study was the very low error rate. The false positive rate was as low as 0% and 5%. None of the results, however, were presented for all three subjects. Yom-Tov and Inbar [42] report 63.2% average classification accuracy (three subjects) for the distinction of real left- and right-finger movements and left-toe movements. Ebrahimi *et al.* [11] consider the mental tasks “mental counting” and imagined left and right index finger movements. Using TFSC, they obtain error rates of 25%, 30%, and 27% for the best session of three subjects. A session comprises three 1-min recordings.

Apart from the system of Anderson, achieving 85% for one subject, the performance of our method is in the range of the accuracies reported in the other studies. It is difficult, however, to directly compare the results from our study and these four studies, as the recording equipments, recording and classification protocols, and the mental tasks considered are different. In addition, the amount of data and the amount of training the subjects had before participating in the BCI experiments is different for the different studies.

In future studies, we would like to test the performance of these features in an online system, providing feedback to the user. Studies with motor-disabled individuals are necessary to confirm that for disabled subjects results similar to these for healthy subjects can be achieved.

IX. CONCLUSION

We are aware that a small sample size does not allow for statistical conclusions regarding the general performance of synchronization estimates for classifying mental tasks. Yet, with this study, we demonstrate that synchronization measures are relevant for classifying mental tasks and show new possibilities for future BCI research. We believe that the study of synchronization can improve the development of BCIs. Further studies are needed to fully exploit its capacities in this context, but these first results are promising. The PLV may be specially suited, because of its fast computation, needed for online feedback.

ACKNOWLEDGMENT

The authors would like to thank the reviewers for their valuable comments, J. del R. Millán and S. Chiappa for providing the data, and the subjects for their voluntary participation in the experiments.

REFERENCES

- [1] J. R. Wolpaw, N. Birbaumer, W. J. Heetderks, D. J. McFarland, P. H. Peckham, G. Schalk, E. Donchin, L. A. Quatrano, C. J. Robinson, and T. M. Vaughan, “Brain-computer interface technology: A review of the first international meeting,” *IEEE Trans. Rehab. Eng.*, vol. 8, pp. 164–173, June 2000.
- [2] I. Wickelgren, “Tapping the mind,” *Science*, vol. 299, pp. 496–499, 2003.
- [3] T. Vaughan, W. Heetderks, L. Trejo, W. Rymer, M. Weinrich, M. Moore, A. Kübler, B. Dobkin, N. Birbaumer, E. Donchin, E. Wolpaw, and J. Wolpaw, “Brain-computer interface technology: A review of the second international meeting,” *IEEE Trans. Neural Syst. Rehab. Eng.*, vol. 11, pp. 94–109, June 2003.
- [4] G. Pfurtscheller and C. Neuper, “Motor imagery and direct brain-computer communication,” *Proc. IEEE*, vol. 89, pp. 1123–1134, July 2001.
- [5] W. Penny, S. Roberts, and M. Stokes, “Imagined hand movements identified from the EEG mu-rhythm,” Dept. Elect. Eng., Imperial College, London, U.K., Tech. Rep., 1998.
- [6] C. Anderson, E. Stolz, and S. Shamsunder, “Discriminating mental tasks using EEG represented by AR models,” in *Proc. IEEE Engineering in Medicine and Biology Annu. Conf.*, Sept. 1995.
- [7] A. Schlögl, G. Pfurtscheller, and B. Schack, “Single-trial EEG analysis using an adaptive autoregressive model,” in *Proc. 4th Int. Symp. Central Nervous Monitoring*, Sept. 1996.
- [8] E. Curran, P. Sykacek, S. Roberts, W. Penny, M. Stokes, I. Johnsrude, and A. Owen, “Cognitive tasks for driving a brain computer interfacing system: a pilot study,” *IEEE Trans. Neural Syst. Rehab. Eng.*, vol. 12, pp. 48–54, Mar. 2004.
- [9] S. Roberts, W. Penny, and I. Rezek, “Temporal and spatial complexity measures for EEG-based brain-computer interfacing,” *Med. Biol. Eng. Comput.*, vol. 37, no. 1, pp. 93–99, 1998.
- [10] C. Guger, H. Ramoser, and G. Pfurtscheller, “Real-time EEG analysis with subject-specific spatial patterns for a brain-computer interface,” *IEEE Trans. Rehab. Eng.*, vol. 8, pp. 447–456, Dec. 2000.
- [11] T. Ebrahimi, J. Vesin, and G. Garcia, “Brain-computer interface in multimedia communication,” *IEEE Signal Process Mag.*, vol. 20, pp. 14–24, Jan. 2003.
- [12] E. Rodriguez, N. George, J. Lachaux, J. Martinerie, B. Renault, and F. Varela, “Perception’s shadow: Long-distance synchronization of human brain activity,” *Nature*, vol. 397, pp. 430–433, Feb. 1999.
- [13] P. Nunez, R. Srinivasan, A. Westdorp, R. Wijesinghe, D. Tucker, and P. C. R. B. Silberstein, “EEG coherency I: Statistics, reference electrode, volume conduction, laplacians, cortical imaging, and interpretation at multiple scales,” *Electroencephalogr. Clin. Neurophysiol.*, vol. 103, pp. 499–515, 1997.
- [14] C. Gerloff, J. Richard, J. Hadley, A. Schulman, M. Honda, and M. Hallett, “Functional coupling and regional activation of human cortical motor areas during simple, internally paced and externally paced finger movements,” *Brain*, vol. 121, pp. 1513–1531, 1998.
- [15] J. Sarnthein, H. Petsche, P. Rappelsberger, G. Shaw, and A. von Stein, “Synchronization between prefrontal and posterior association cortex during human working memory,” *Proc. Natl. Acad. Sci.*, vol. 95, pp. 7092–7096, 1998.
- [16] B. Schack, P. Rappelsberger, C. Anders, S. Weiss, and E. Möller, “Quantification of synchronization processes by coherence and phase and its application in analysis of electrophysiological signals,” *Int. J. Bif. Chaos*, vol. 10, no. 11, pp. 2565–2586, 2000.
- [17] A. Delorme and S. Makeig, “EEG changes accompanying learning regulation of the 12-Hz EEG activity,” *IEEE Trans. Rehab. Eng.*, vol. 11, pp. 133–136, June 2003.
- [18] M. Hoke, K. Lehnertz, C. Pantev, and B. Lütkenhöner, *Brain Dynamics, Progress and Perspectives*, ser. Brain Dynamics. Berlin, Germany: Springer-Verlag, 1989, ch. Spatiotemporal Aspects of Synergetic Processes in the Auditory Cortex as Revealed by the Magnetoencephalogram.
- [19] J. Lachaux, E. Rodriguez, J. Martinerie, and F. Varela, “Measuring phase synchrony in brain signals,” *Human Brain Map*, vol. 8, pp. 194–208, 1999.
- [20] F. Mormann, K. Lehnertz, P. David, and C. Elger, “Mean phase coherence as a measure for phase synchronization and its application to the EEG of epilepsy patients,” *Physica D*, vol. 144, pp. 358–369, 2000.
- [21] J. Lachaux, E. Rodriguez, M. Le Van Quyen, A. Lutz, J. Martinerie, and F. Varela, “Studying single-trials of phase synchronous activity in the brain,” *Int. J. Bif. Chaos*, vol. 10, no. 10, pp. 2429–2439, 2000.

- [22] M. Le Van Quyen, J. Foucher, J. Lachaux, E. Rodriguez, A. Lutz, J. Martinerie, and F. Varela, "Comparison of hilbert transform and wavelet methods for the analysis of neuronal synchrony," *J. Neurosci. Meth.*, vol. 111, pp. 83–98, 2001.
- [23] M. Le Van Quyen, J. Martinerie, V. Navarro, M. Baulac, and F. Varela, "Characterizing neurodynamic changes before seizures," *J. Clin. Neurophysiol.*, vol. 18, no. 3, pp. 191–208, 2001.
- [24] J. Bhattacharya, "Reduced degree of long-range phase synchrony in pathological human brain," *Acta Neurobiol. Exp.*, vol. 61, pp. 309–318, 2001.
- [25] J. Bhattacharya, H. Petsche, U. Feldmann, and B. Rescher, "EEG gamma-band phase synchronization between posterior and frontal cortex during mental rotation in humans," *Neurosci. Lett.*, vol. 311, pp. 29–32, 2001.
- [26] J. Bhattacharya and H. Petsche, "Shadows of artistry: Cortical synchrony during perception and imagery of visual art," *Cogn. Brain Res.*, vol. 13, pp. 179–186, 2002.
- [27] E. Gysels, M. Le Van Quyen, J. Martinerie, P. Boon, K. Vonck, I. Lemahieu, and R. Van de Walle, "Long-term evaluation of synchronization between scalp EEG signals in partial epilepsy," in *Proc. 9th Int. Conf. Neural Information Processing*, vol. 3, Nov. 2002, pp. 1495–1498.
- [28] F. Mormann, T. Kreuz, R. Andrzejak, P. David, K. Lehnertz, and C. Elger, "Epileptic seizures are preceded by a decrease in synchronization," *Epilepsia*, vol. 53, pp. 173–185, 2003.
- [29] M. van Putten, "Proposed link rates in the human brain," *J. Neurosci. Meth.*, vol. 127, pp. 1–10, 2003.
- [30] R. Quiroga, A. Kraskov, T. Kreuz, and P. Grassberger, "Performance of different synchronization measures in real data: A case study on electroencephalographic signals," *Phys. Rev. E, Stat. Phys. Plasmas Fluids Relat. Interdiscip. Top.*, vol. 65, no. 041903, 2002.
- [31] N. Birbaumer, A. Kübler, N. Ghanayim, T. Hinterberger, J. Perelmouter, J. Kaiser, I. Iversen, B. Kotchoubey, N. Neumann, and H. Flor, "The thought translation device (TTD) for completely paralyzed patients," *IEEE Trans. Rehab. Eng.*, vol. 8, pp. 190–193, June 2000.
- [32] A. Gevins, C. Yeager, G. Zeitlin, S. Ancoli, and M. Dedon, "On-line computer rejection of EEG artifact," *Electroencephalogr. Clin. Neurophysiol.*, vol. 42, pp. 267–274, 1977.
- [33] T.-P. Jung, S. Makeig, C. Humphries, T. Lee, M. McKeown, V. Iragui, and T. Sejnowski, "Removing electroencephalographic artifacts by blind source separation," *Psychophysiology*, vol. 37, pp. 163–178, 2000.
- [34] A. Schlögl, P. Anderer, M.-J. Barbanoj, G. Klösch, G. Gruber, J. Lorenzo, O. Filz, M. Koivuluoma, I. Rezek, S. Roberts, A. Värri, P. Rappelsberger, G. Pfurtscheller, and G. Dorffner, "Artefact processing of the sleep EEG in the 'SIESTA' project," in *Proc. EM-BEC*, vol. 1, 1999, pp. 1644–1645.
- [35] F. Perrin, J. Pernier, O. Bertrand, and J. Echallier, "Spherical splines for scalp potential and current density mapping," *Electroencephalogr. Clin. Neurophysiol.*, vol. 72, pp. 184–187, 1989.
- [36] —, "Corrigendum EEG 02 274," *Electroencephalogr. Clin. Neurophysiol.*, vol. 76, p. 565, 1990.
- [37] B. Boashash, "Estimating and interpreting the instantaneous frequency of a signal—Part 1: Fundamentals," *Proc. IEEE*, vol. 80, pp. 520–538, Apr. 1992.
- [38] A. Oppenheim and R. Schaffer, *Discrete-Time Signal Processing*. Englewood Cliffs, NJ: Prentice-Hall, 1999, ch. 11.
- [39] M. Rosenblum, A. Pikovsky, J. Kurths, C. Schäfer, and P. Tass, *Handbook of Biological Physics*. Amsterdam, The Netherlands: Elsevier, 2001, vol. 4, ch. Phase synchronization: From theory to data analysis, pp. 279–321.
- [40] C. Anderson, "Effects of variations in neural network topology and output averaging on the discrimination of mental tasks from spontaneous electroencephalogram," *J. Intell. Syst.*, vol. 7, no. 1–2, pp. 165–190, 1997.
- [41] J. del R. Millán, J. Mouriño, F. Babiloni, F. Cincotti, M. Varsta, and J. Heikkonen, "Local neural classifier for EEG-based recognition of mental tasks," in *Proc. IEEE-INNS-ENNS Int. Joint Conf. Neural Networks*, vol. 3, July 2000, pp. 3632–3636.
- [42] E. Yom-Tov and G. Inbar, "Feature selection for the classification of movements from single movement-related potentials," *IEEE Trans. Neural. Syst. Rehab. Eng.*, vol. 10, pp. 170–177, Sept. 2002.

Elly Gysels received the degree in physics engineering from Ghent University, Ghent, Belgium, in 2001. She is currently working toward the Ph.D. degree in brain-machine interfaces at the Swiss Center for Electronics and Microtechnology, Neuchâtel, Switzerland.

She worked for one year as a Scientific Collaborator on the anticipation of epileptic seizures at the Department of Electronics and Information Systems, Ghent University in collaboration with the Reference Center for Refractory Epilepsy, Department of Neurology, Ghent University Hospital, Belgium, and the Neurodynamics Group, Hôpital de la Salpêtrière, Paris, France.

Patrick Celka received the degree in physical sciences from the Catholic University of Louvain-la-Neuve, Louvain-la-Neuve, Belgium, in 1987, and the M.S. degree in information and signal processing and the Ph.D. degree from the Swiss Federal Institute of Technology (EPFL), Lausanne, Switzerland, in 1993 and 1995, respectively.

From 1995 to 1999, he was a Senior Research Assistant at the Signal Processing Laboratory, EPFL. From 1999 to 2001, he was leading a biomedical project dealing with the automatic detection/classification of EEG seizures in the newborn at the Signal Processing Research Centre, Queensland University of Technology, Brisbane, Australia. After working three years at the Swiss Center for Electronics and Microtechnology, Neuchâtel, Switzerland, he is now with Griffith University, Australia. His research interests include nonlinear dynamical systems theory, nonlinear signal and system modeling and identification, chaos theory and its application, nonlinear adaptive algorithms, and biomedical engineering.